Core and edge toroidal rotation study in JT-60U

M. Yoshida, Y. Sakamoto, M. Honda, Y. Kamada, H. Takenaga, N. Oyama, H. Urano, and the JT-60 team

Japan Atomic Energy Agency, Naka, Ibaraki-ken, 311-0193 Japan

e-mail contact of main author : yoshida.maiko@jaea.go.jp

Abstract. Relation between the toroidal rotation velocities (V_t) in the core and edge regions has been investigated in H-mode and internal transport barrier (ITB) plasmas with small external torque input from the viewpoint of momentum transport. Main results are as follows: (i) the core-V_t gradually varies with timescale of ~ 20 ms after a rapid change in the edge-V_t at L-H transition. This timescale of ~20 ms is comparable to a transport time scale of $\sim L^2/\chi_\phi \sim L/V_{conv}$. Here χ_ϕ, V_{conv} and L are the momentum diffusivity, the convection velocity and the distance from edge, respectively. In steady state, a linear correlation between the core- and edge-V_t is observed in H-mode plasmas when the ion pressure gradient (∇P_i) is small. This relation between core- and edge-V_t is also explained by the momentum transport. (ii) The V_t profiles with the ∇P_i being large have been reproduced in the region of r/a~0.20-0.7 by considering a residual stress term "$\Pi_{res}=\alpha_k\chi_\phi\nabla P_i$" proposed in this paper. By using this formula, the V_t profiles have been reproduced over a wide range of plasma conditions. (iii) parameter dependencies of the edge-V_t are investigated at constant ripple loss power (P_{RP}), ripple amplitude and the plasma current (I_p). A reduction in the CTR-rotation is observed with degreasing the ion temperature gradient (∇T_i). (iv) A reduction in χ_ϕ has been observed in the ITB region. The momentum diffusivity reduces to the almost same level of χ_i in the ITB region.

1. Introduction

In future burning plasmas such as ITER and DEMO, the external torque input is expected to be small [1]. Understanding the physical mechanism determining the toroidal rotation velocity (V_t) profile and its control are a critical issue in ITER and DEMO from the viewpoint of the confinement improvement [2], MHD stability [3] and impurity accumulation [4]. Therefore, it is essential to understand the rotation mechanisms from the core to edge regions under the condition of small torque input. In this paper, we report four topics: (i) relation between the edge-V_t and the core-V_t, where the edge-V_t and the core-V_t mean the rotation at r/a~0.8 and r/a~0.5, respectively, (ii) the intrinsic rotation in the core region (r/a<0.7), (iii) properties of V_t in the edge region (r/a~0.8-0.9), and (iv) the momentum transport inside internal transport barriers (ITBs) under the condition of small torque input.

In this paper, for understanding the relation between the edge-V_t and the core-V_t with small torque input, we investigate how the edge-V_t affects the core-V_t temporally by means of the measurement of V_t at L-H and H-L transitions. And a relation between the edge-V_t and the core-V_t in steady state is identified by plasma parameter scans such as neutral beam (NB) heating power (P_{NB}), electron density (n_e) and the ripple amplitude by varying the toroidal magnetic field (B_T) with BAL-NBI. After the understanding of the relation between the core-V_t and the edge-V_t, we focus on the core-V_t and the edge-V_t individually. Concerning the core-V_t, it was reported in the previous studies [5] that the V_t profiles, which could not be reproduced by the toroidal momentum diffusivity (χ_ϕ) and the convection velocity (V_{conv}), were found, when the ion pressure gradient (∇P_i) became large in JT-60U. The question of how these V_t profiles are reproduced has remained. In this paper, the V_t profiles with the ∇P_i being large have been reproduced by considering a residual stress term. We propose the formula as "$\Pi_{res}=\alpha_k\chi_\phi\nabla P_i$" based on the experimental results in [5]. In addition, χ_ϕ and V_{conv} have been evaluated in an ITB plasma for the first time. For evaluation of χ_ϕ and V_{conv}, we use the transient transport analysis with off-axis perpendicular-NBs (PERP-NBs), which enhances the CTR-rotation by the fast ion losses due to the toroidal field ripple in the peripheral region [6-8]. The heating power of the off-axis PERP-NBs is mainly deposited outside the ITB

region, and the heating power of the off-axis PERP-NBs is much smaller than the total heating power (~11% of the total input power). These advantages enable us to perform the modulation experiment in the ITB plasma. Concerning the edge-V_t, parameter dependencies of the edge-V_t are investigated at constant ripple loss power (P_{RP}), ripple amplitude and the plasma current (I_p).

2. Experiment

Experiments were conducted in the JT-60U tokamak where NBs of various injection geometries are installed. They consist of two tangential beams directing the same direction as that of the plasma current (CO-NBs), two tangential beams directing opposite to the plasma current (CTR-NBs) and seven near perpendicular (CO- and CTR-PERP) beams. Five of the PERP-NBs are almost on-axis deposition, and other two PERP-NBs are off-axis. The injection angle of tangential beams is 36 degree and that of PERP-NBs is 75 degree with respect to the magnetic axis. The deuterium beam acceleration energy is about 85 keV, and the input power per injected unit is about 2 MW.
The χ_ϕ and V_{conv} are evaluated from the toroidal momentum balance equation written as,

$$m_i \frac{\partial n_i V_t}{\partial t} = -\nabla \cdot \left\{ -m_i \chi_\phi \frac{\partial n_i V_t}{\partial r} + m_i V_{conv} n_i V_t \right\} + S, \qquad (1)$$

where m_i, n_i, M and S are the ion mass, the ion density, the toroidal momentum flux and the toroidal momentum source, respectively [7,8]. In order to evaluate the profiles of χ_ϕ and V_{conv}, the transient transport of toroidal momentum is conducted by using modulated injection of PERP-NBs, which enhances CTR rotation by the fast ion losses due to the toroidal field ripple in the peripheral region of the plasma [6]. In this report, ions are defined as the main (deuterium) and impurity ions, assuming that the toroidal rotation velocities of the main ions are the same as that of the carbon impurity ions, which is measured by the charge exchange recombination spectroscopy (CXRS). The negative sign of V_t and positive sign of one designate CTR- (in the opposite direction to the plasma current, I_p) and CO- (in the direction to I_p) directed rotation, respectively. The ripple amplitude defined as $(B_{max}-B_{min})/(B_{max}+B_{min})$, is about 0.15, 0.3, 1% (averaged over the toroidal direction) at r/a~0.3, 0.5 and 0.9 at B_T=2.5 T, respectively.

3. Correlation between the core and edge rotations

An impact of the edge-V_t to the core-V_t has been investigated through L-H and H-L transitions. Figure 1(a) shows waveforms of V_t at r/a~0.47 and 0.9 and D_α signal at outer diverter (I_P=1.0 MA, B_T=3.0 T, the absorbed power, P_{ABS}=8 MW). L-H transition occurs at t~5.526 s and H-L back transition occurs at t~5.569 s as denoted by the D_α signal. At first V_t at the edge (r/a~0.9) changes rapidly, and then V_t at the core (r/a~0.47) gradually changes at both transitions. The slower evolution of T_i at r/a~0.9 and the line integrated-density at high filed side (nl_{edge}), which passes through the position of r/a~0.8, are observed compared to the evolution of V_t at r/a~0.9 as shown in Figs. 1(b) and 1(c). The core-V_t affected by the edge-V_t varies with the time scale of ~20 ms after the L-H transition. This value almost agrees with a transport time scale of $\sim L^2/\chi_\phi \sim L/V_{conv}$. Here L is the distance from the edge (~0.5 m). The toroidal momentum diffusivity (χ_ϕ) and the convection velocity (V_{conv}) are given by the scaling in [8]. The ion temperature at r/a~0.6 is about 3 keV in this plasma. In this regime, χ_ϕ and V_{conv} can be predicted about 15 m^2/s and -18 m/s, respectively, by referring the scaling in [8]. Then L^2/χ_ϕ and L/V_{conv} are about 19 ms and 33 m, respectively.

The relation between the core-V_t (r/a~0.47) and the edge-V_t (r/a~0.9) at L-H and H-L transitions shown in Fig. 1 is plotted in Fig. 2(a). Open symbols indicate the data at the transition. At both transitions, first, the edge-V_t varies with the core-V_t being constant, and

then, the core-V_t varies with the edge-V_t. On the other hand, T_i at the core and edge regions varies nearly simultaneously as shown in Fig. 2(b). These data mean that the behavior of V_t is different from that of T_i having simultaneity or profile stiffness. Thus, the V_t profile is not characterized by the profile stiffness but determined by the momentum transport coefficients (χ_ϕ and V_{conv}) evaluated by the transient transport analysis.

In order to understand characteristics of the V_t structure, the correlation between the core- and edge-V_t have been identified in steady state BAL-NBs injected H-mode plasmas. Shown in Fig. 3 is the relation between the core-V_t (r/a~0.3 and 0.5) and edge-V_t (r/a~0.8) in the scans of the density ($\bar{n}_e$=1.5-3.3×10^{19} m^{-3}), the heating power (P_{NB}=6.1-13.1 MW) and the toroidal magnetic field (B_T=1.7-3.8 T). In the region r/a~0.5-0.7, the intrinsic rotation induced by ∇P_i is considered to be negligibly small (discussed in Sec. 4). And the ripple loss of fast ion, which can induce the CTR-rotation, is localized at r/a>0.8 (discussed in Sec. 5). When there is no torque, the momentum transport equation (1) can be described as $V_{conv}/\chi_\phi=(1/V_t)\partial V_t/\partial r$ in steady state. Solid line in Fig. 3 indicates the prediction calculated from the momentum transport equation at RV_{conv}/χ_ϕ=2.4. Here R=3.44 m is the plasma major radius. The value RV_{conv}/χ_ϕ=2.4 is given by the scaling in [8]. From these results, the V_t structure in the region r/a~0.5-0.8, where the ion pressure gradient is small (discussed in Sec. 5), is determine by the momentum transport equation of (1) using χ_ϕ and V_{conv} from the transient transport analysis.

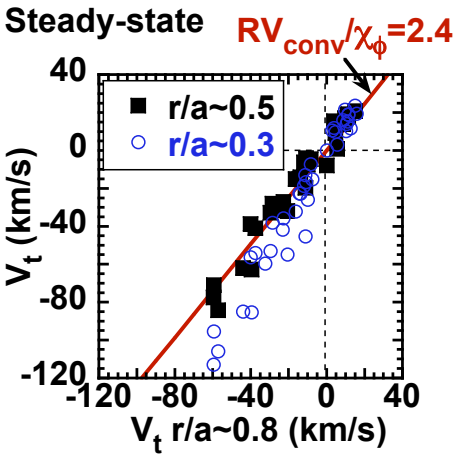

Fig. 3 Relations between the core (r/a=0.3 and 0.5) and edge V_t (r/a=0.8) at steady state in the scans of density ($\bar{n}_e$=1.5-3.3×10^{19} m^{-3}), the heating power (P_{NB}=6.1-13.1 MW) and B_T (B_T=1.7-3.8 T).

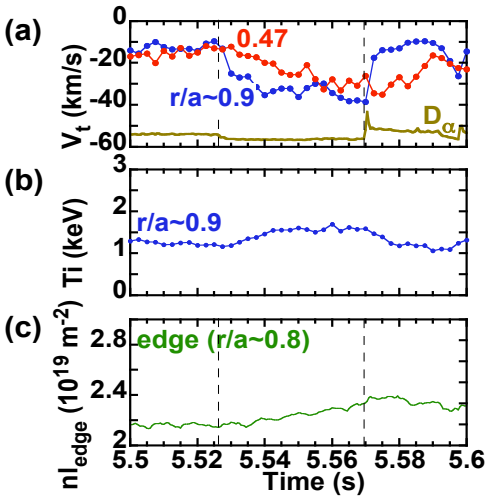

Fig. 1 Waveforms of (a) the toroidal rotation velocity (V_t) at r/a~0.47 and 0.9 and D_α signal, (b) the ion temperature (T_i) at r/a~0.9 and (c) the line-integrated electron density through the edge (r/a~0.8) (nl_{edge}) at L-H and H-L transitions (I_P=1.0 MA, B_T=3.0 T, P_{NB}=11.4 MW).

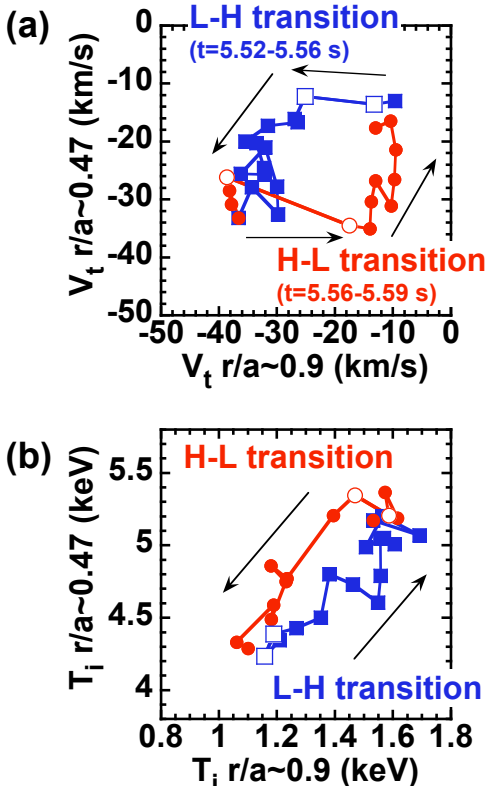

Fig. 2 (a) Relation of the core-and edge-V_t and (b) relation of the core-and edge-T_i at L-H transition and H-L transitions (the same discharge as in Fig. 1). Open symbols indicate the data at transitions.

4. Core-rotation with the intrinsic rotation

In Fig. 3, data at r/a~0.3 become to more negative (CTR-direction). This result mainly comes from the effect of the intrinsic rotation with the pressure gradient (∇P_i) being steeper. In the previous studies [5], we reported that the V_t profiles, which cannot be reproduced by only the momentum transport model (1), indicate the existence of the intrinsic rotation. In that case, the local value of intrinsic rotation velocity increases with increasing the local ∇P_i. And the relation between the intrinsic rotation and ∇P_i does not strongly depend on χ_ϕ [5].

In this section, the V_t profiles have been reproduced by considering the diffusive, convective and a residual term (Π_{res}). We have proposed the residual stress term as "$\Pi_{res}=\alpha_{k1}\chi_\phi \nabla P_i$" (assuming α_{k1} is a constant in radius). This formula is proposed based on the above-mentioned experimental results (the intrinsic rotation increases with increasing ∇P_i and this tendency is almost the same over a wide range of χ_ϕ) and a thought that χ_ϕ is adopted as a turbulent state of the plasma. Then the momentum transport equation is written as

$$m_i \frac{\partial n_i V_t}{\partial t} = -\nabla \cdot \left\{ -m_i \chi_\phi \frac{\partial n_i V_t}{\partial r} + m_i V_{conv} n_i V_t + \Pi_{res} \right\} + S \qquad (2)$$

$$\Pi_{res}=\alpha_{k1}\chi_\phi \nabla P_i \,.$$

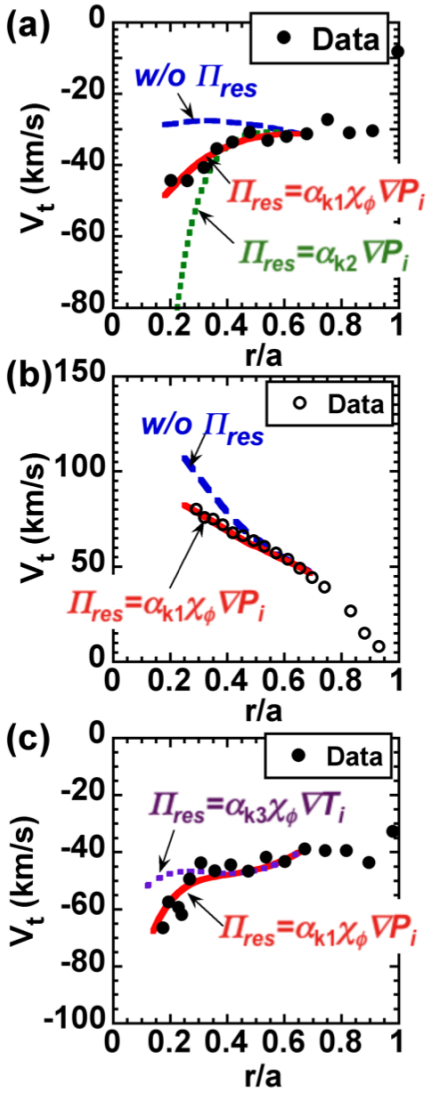

Fig. 4 (a) Profiles of the measured V_t, the calculated V_t with $\Pi_{res}=\alpha_{k1}\chi_\phi \nabla P_i$, $\Pi_{res}=\alpha_{k2}\nabla P_i$ and without Π_{res} (H-mode with BAL-NBs). (b) Profiles of the measured V_t, the calculated V_t with $\Pi_{res}=\alpha_{k1}\chi_\phi \nabla P_i$ and without Π_{res} in CO-rotating H-mode plasma. (c) Profiles of the measured V_t, the calculated V_t with $\Pi_{res}=\alpha_{k1}\chi_\phi \nabla P_i$ and $\Pi_{res}=\alpha_{k3}\chi_\phi \nabla T_i$ (L-mode).

In order to test the model, we calculate the V_t profiles with and without Π_{res} in various plasmas as shown in Fig. 4. Figure 4(a) illustrates the measured V_t profile (solid circles) in an H-mode plasma (I_P=1.2 MA, B_T=2.6 T, P_{ABS}=5.6 MW, BAL-NBs). The dashed line and the solid line show the calculated V_t by the momentum transport model without and with Π_{res}, respectively. The calculated V_t without Π_{res} (dashed line) deviates from the measured V_t. On the other hand, the V_t profile is reproduced by considering $\Pi_{res}=\alpha_{k1}\chi_\phi \nabla P_i$ (solid line). In this plasma, we set $\alpha_{k1}=1.5\times10^{-7}$ m^{-1}s, and the units of α_{k1} is m^{-1}s. When we use another formula $\Pi_{res}=\alpha_{k2}\nabla P_i$ instead of $\Pi_{res}=\alpha_{k1}\chi_\phi \nabla P_i$, the V_t profile is not reproduced as shown in dotted line in Fig. 4(a). We also adopt the formula $\Pi_{res}=\alpha_{k1}\chi_\phi \nabla P_i$ for a CO-rotating H-mode plasma as shown in Fig. 4(b) (I_P=1.2 MA, B_T=2.8 T, P_{ABS}=8.4 MW). By using the term $\Pi_{res}=\alpha_{k1}\chi_\phi \nabla P_i$ ($\alpha_{k1}=1.0\times10^{-7}$ m^{-1}s), a good agreement is observed between the measured V_t and calculated V_t. We attempt to reproduce V_t profiles using ∇T_i instead of ∇P_i, i.e. "$\Pi_{res}=\alpha_{k3}\chi_\phi \nabla T_i$" for the dataset. Although the increase in ∇T_i generally accompanies with the increase in ∇P_i, some V_t profiles cannot be

reproduced by $\Pi_{res}= \alpha_{k3}\chi_\phi \nabla T_i$. One example is shown in Fig. 4(c) (I_P=1.5 MA, B_T=3.8 T, P_{ABS}=6.4 MW, L-mode plasma). The calculated V_t profile by using $\Pi_{res}= \alpha_{k3}\chi_\phi \nabla T_i$ is shown by the dotted line. Here again, the solid line and solid circles denote the calculated V_t profile by using $\Pi_{res}=\alpha_{k1}\chi_\phi \nabla P_i$ (α_{k1}=2.5×10^{-7} m^{-1}s) and measurement, respectively. The V_t profile is reproduced by using $\Pi_{res}=\alpha_{k1}\chi_\phi \nabla P_i$ rather than $\Pi_{res}= \alpha_{k3}\chi_\phi \nabla T_i$. We calculate V_t profiles by using $\Pi_{res}= \alpha_{k1}\chi_\phi \nabla P_i$, $\Pi_{res}= \alpha_{k3}\chi_\phi \nabla T_i$ and $\Pi_{res}= \alpha_{k2} \nabla P_i$ for wide ranges of plasma parameters (I_P=1.0-1.8 MA, B_T=2.5-3.8 T, P_{NB}=6-11 MW, β_N~1-1.6, CO-rotating and CTR-rotating, standard L-mode and H-mode plasmas), and we identify that the best fit through the plasmas is obtained with $\Pi_{res}=\alpha_{k1}\chi_\phi \nabla P_i$. We set the value of α_{k1} every discharge and the value of α_{k1} is in the range from 1.0×10^{-7} to 3.0×10^{-7} m^{-1}s for this series of discharges.

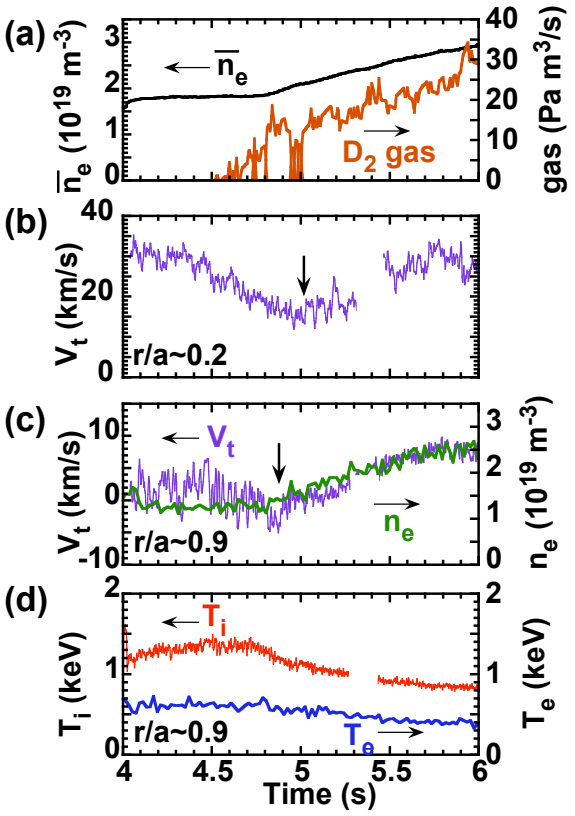

Fig. 5 Waveforms of (a) the line averaged electron density ($\bar{n}_e$) and D_2 gas, (b) V_t r/a~0.2, (c) V_t and n_e at r/a~0.9, and (d) T_i and T_e at r/a~0.9 in an H-mode plasma (I_P=1.2 MA, B_T=2.26 T, P_{NB}=7.4 MW, V_p=74 m^3).

5. Edge-rotation properties

As shown in Sec. 3, the core-V_t has a relation with the edge-V_t. Therefore studies on the edge-V_t properties are indispensable for elucidation and control of the core-V_t. In this section, the properties of the edge-V_t are investigated in H-mode plasmas with small torque input, where CO- and CTR-tangential NBs are injected with the almost same power and same energy, and 2 units of PERP-NBs are injected.

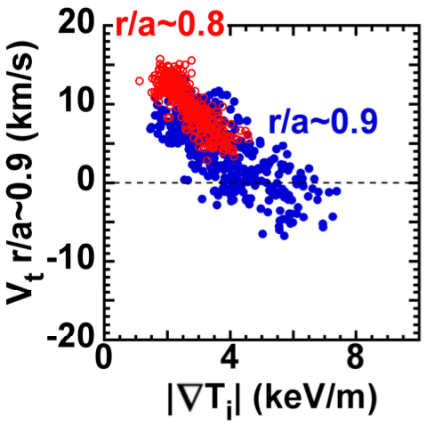

Fig. 6 Relation of the edge-V_t (r/a~0.8, 0.9) and the ion temperature gradient (∇T_i) (the same discharge as in Fig. 5)

Shown in Fig. 5(a) is the time traces of data of the line averaged electron density ($\bar{n}_e$) and D_2 gas in an H-mode plasma (I_P=1.2 MA, B_T=2.26 T, P_{ABS}=5.2 MW, the plasma volume, V_p=74 m^3). When a large amount of D_2 gas of ~10-30 Pa m^3/s was puffed during NB injection, $\bar{n}_e$ and n_e at r/a~0.9 increased as shown in Figs. 5(a) and 5(c). The toroidal rotation velocity at r/a~0.9 starts to increases in the CO-direction after n_e starts to increase as shown in Fig. 5(c). The timescale of the increase in V_t is similar to that in n_e. Simultaneously, T_i and T_e at r/a~0.9 decrease with increasing n_e at constant heating power (Fig. 5(d)). Waveforms of V_t at r/a~0.2 is illustrated in Fig. 5(b). The starting time of the change in V_t toward the CO-direction is shown by the dashed line and arrow for each radial position (Figs. 5(b) and 5(c)). One can see the change in V_t starts from the edge region, when the density increases by increasing gas puff rate. The relation between V_t and ∇T_i at r/a~0.8 and 0.9 is plotted in Fig. 6. The data come from the

waveforms at 4.8-6.0 s in Fig. 5. Here ∇T_i is defined as the T_i gradient across the H-mode pedestal (r/a~0.8-1 or ~0.9-1), i.e. $\nabla T_i \equiv \Delta T_i / L_{edge}$. Here ΔT_i is the difference in T_i between r/a~0.8 or 0.9 to 1, and L_{edge} is the distance from r/a=0.8 or 0.9 to 1. The toroidal rotation velocity linearly increases in the CO-direction with decreasing ∇T_i.

The V_t profile is determined by various mechanisms, such as (i) collisional momentum transfer by NBs, (ii) the radial current torque (jxB torque) [9], (iii) the inward electric field through the prompt fast ion loss [6], (iv) NTV torque [10] ((i)-(iv) are included in the fourth term in the r.h.s of eq. (2)), (v) Residual stress [11] (the third term in r.h.s. of eq (2)), (vi) the change in the momentum transport (the first and second terms in r.h.s. of eq (2)) and so on. We investigate parameter dependences of the edge-V_t focusing on momentum source or flux (the third and fourth terms in r.h.s. of eq (2)) by using the n_e scan in Fig. 3. Typical V_t profiles at low, middle and high density is shown in Fig. 7 ($\bar{n}_e$~1.8×10^{19} m^{-3}, 2.2×10^{19} m^{-3}, 3.0×10^{19} m^{-3}). In the case of $\bar{n}_e$~3.0×10^{19} m^{-3}, a large amount of D_2 gas of 10-30 Pa m^3/s was puffed during NB injection.

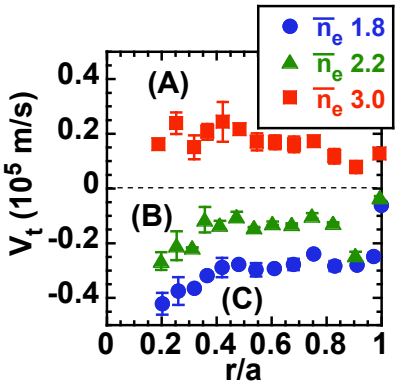

Fig. 7 Profiles of V_t at low, middle and high density ($\bar{n}_e$~1.8×10^{19} m^{-3}, 2.2×10^{19} m^{-3}, 3.0×10^{19} m^{-3}).

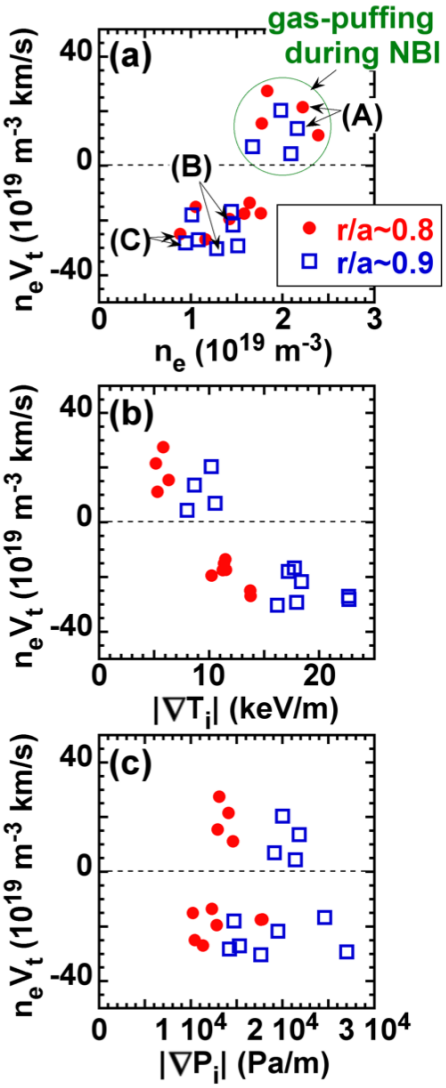

Fig. 8 Relation between n_eV_t and (a) n_e, (b) $|\nabla T_i|$ and (c) $|\nabla P_i|$ at the peripheral region in the density scan (P_{RP}~0.9 MW, I_p=1.2 MA, B_T~2.5 T and P_{ABS}~6 MW).

In order to minimize the effects of (i), (iii) and (vi) mentioned above, we performed the n_e scan ($\bar{n}_e$~1.8-3.3×10^{19} m^{-3}) with small torque input (BAL-NBI), at constant ripple loss power (P_{RP}) and I_p (P_{RP}~0.9 MW, I_p=1.2 MA, B_T~2.5 T and P_{ABS}~6 MW). Also the maximum ripple amplitude is kept constant of ~1%. The CTR-rotation reduces with increasing n_e, and the CO-rotation is observed at high density with gas puffing during NBI as shown in Fig. 8(a). The V_t profiles denoted (A)-(C) are shown in Fig. 7. Figure 8(b) shows the relation between n_eV_t and $|\nabla T_i|$ at r/a~0.8 and 0.9. A reduction in the CTR-rotation is observed with degreasing $|\nabla T_i|$ (or T_i), because T_i decreases with increasing n_e in this dataset. A clear dependency on ∇P_i was not observed at edge region (r/a~0.8, 0.9) as shown in Fig. 8(c). Here ∇T_i and ∇P_i are defined as the T_i and P_i gradients across the H-mode pedestal (r/a~0.8-1 or r/a~0.9-1), respectively. This result (the CO-rotation relates ∇T_i rather than ∇P_i) is different from the result in the core region discussed in Sec. 4. One of the differences between the core and the edge condition is the magnitude of the magnetic field ripple; small ripple in the core region (~0.15% at r/a~0.3) and larger ripple in the edge region (~1% at r/a~0.9). The

dependence of the edge-V_t on ∇T_i might correlate with the magnetic field ripple.

Recently jxB torque has been calculated with the orbit-following Monte Calro code (OFMC). We calculate jxB torque for three discharges shown in Fig. 7. From the calculation, jxB torque in the edge region r/a~0.8-1, which is mainly due to the ripple loss of fast ion, is kept almost constant. Although jxB torque decreases with increasing n_e in the region of 0.2<r/a<0.8, this change is cancelled by the change in the collisional torque. Therefore, the total external torque input is almost kept constant (0.62-0.77 Nm) even if n_e varies. From these results, we conclude that there is the torques in the CTR-direction, which increases with increasing in ∇T_i in the edge region.

6. Momentum transport inside ITBs

In the previous studies [7,8], the characteristics of the momentum transport in L-mode and H-mode plasmas are mainly discussed. In this section, the relations between χ_ϕ, χ_i and V_{conv} in ITB plasmas are elucidated.

In order to investigate the characteristics of momentum transport and V_t in ITB plasmas, the transient transport analysis was performed. Shown in Figs. 9(a) and 9(b) are the radial profiles of T_i and V_t in positive shear L-mode plasmas comparing the profiles with and without ITB (I_P=1.0 MA, B_T=3.8 T). For the plasma without ITB, 2 units of CO tangential NBs, 2 units of CTR tangential NBs and 2 units of PERP-NBs are injected, resulting P_{ABS}=6.8 MW. For the plasma with ITB, 1 unit of PERP-NBs is added, and the total power is P_{ABS}=8.5 MW. The line averaged electron density is $\bar{n}_e$~1.5-1.6x10^{19} m^{-3}. The elongation at separatrix (κ_x) and the triangularity at separatrix (δ_x) are kept almost constant for this series of discharges (κ_x~1.42-1.45, δ_x~0.3). A T_i-ITB forms around r/a~0.3-0.4.

We performed the transient transport analysis in these two target plasmas. We use the off-axis PERP-NB with small power for modulation (~11% of the total

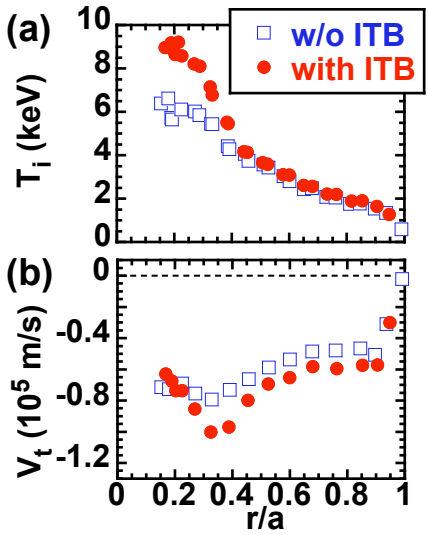

Fig. 9 Radial profiles of (a) the ion temperature (T_i) and (b) V_t. Circles indicate the plasma with ITB, squares indicate the plasma without ITB.

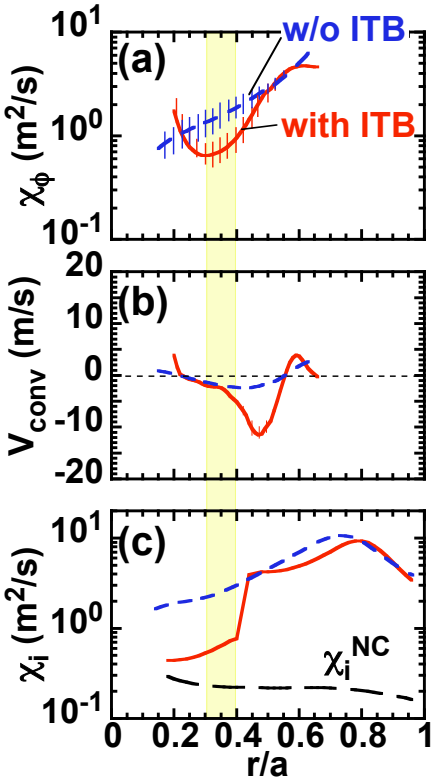

Fig. 10 Profiles of (a) χ_ϕ and (b) V_{conv} obtained from the transient transport analysis. (c) Profiles of the heat diffusivity (χ_i) in L-mode plasmas with and without ITB.

input power) to advantage in the experiment. Moreover, effects of the modulated part of T_i and n_e on the intrinsic rotation, which are ~2% and ~1%, respectively, can be negligible. Thus, we have obtained χ_ϕ and V_{conv} inside the ITB for the first time as shown in Figs. 10(a) and 10(b). Although the heat diffusivity (χ_i) decreases inside the ITB, the ion neoclassical transport level is lower than the observed χ_i in this plasma as shown in Fig. 10(c). The reduction of χ_ϕ in the ITB region has been observed. The momentum diffusivity decreases to the almost same level of χ_i in the ITB region. The convection velocity (V_{conv}) does not change significantly in the ITB region. The ratio of χ_ϕ/χ_i varies from ~0.6 to ~1, and RV_{conv}/χ_ϕ varies from ~ -4 to ~ -13 in the ITB region ($0.3<r/a<0.4$) after the ITB formation.

6. Summary

In this paper, the relation between the toroidal rotation velocity (V_t) in the core and edge regions has been investigated in H-mode plasmas with small external torque input. In order to understand the V_t response, an impact of the edge-V_t to the core-V_t is investigated through L-H and H-L transitions. At both L-H and H-L transitions, at first, the edge-V_t rapidly changes of the order to ~ms. After the L-H transition the core-V_t gradually changes taking about 20 ms. This timescale is comparable to the transport timescale of $\sim L^2/\chi_\phi \sim L/V_{conv}$. The V_t behavior is different from the T_i behavior like profile stiffness at L-H and H-L transitions. Concerning the characteristic of V_t profile in steady state, a linear correlation between the core- and edge-V_t is identified in H-mode plasmas when the ion pressure gradient (∇P_i) is small. The structure is also explained by the momentum transport coefficients (χ_ϕ and V_{conv}). At large ∇P_i, the V_t profiles have been reproduced by considering the residual stress term "$\Pi_{res}=\alpha_k\chi_\phi\nabla P_i$" proposed in this paper. We confirmed the V_t profiles with ∇P_i being large were explained over a wide range of plasma parameters by using this formula (I_P=1.0-1.8 MA, B_T=2.5-3.8 T, P_{NB}=6-11 MW, β_N~1-1.6, CO-rotating and CTR-rotating, standard L-mode and H-mode plasmas). We have found the properties of the edge rotation (r/a~0.8-0.9) at constant I_P, P_{NB}, P_{RP} and ripple amplitude (plasma configuration). The CTR-rotation reduces with degreasing ∇T_i rather than ∇P_i. Finally, the reduction in χ_ϕ has been observed in the ITB region for the first time. The momentum transport diffusivity (χ_ϕ) reduces to almost the same level of χ_i in the ITB region

Acknowledgements

The authors would like to thank Dr P. Diamond, Dr T. S. Hahm, Dr V. Parail and Dr J. D. Callen for their fruitful discussions and suggestions.

References

[1] Special issue on Progress in the ITER Physics Basis [Nucl. Fusion **47**, S18 (2007)].
[2] SAKAMOTO, Y., et al., Nucl. Fusion **41** (2001) 865.
[3] TAKECHI, M., et al., Phys. Rev. Lett. **98**, (2007) 055002.
[4] NAKANO, T., et al., Nucl. Fusion **49**, (2009) 115024.
[5] YOSHIDA, M., et al., Phys. Rev. Lett. **100**, (2008) 105002.
[6] YOSHIDA, M., et al., Plasma Phys. Control. Fusion **48**, (2006) 1673.
[7] YOSHIDA, M., et al., Nucl. Fusion **47**, (2007) 856.
[8] YOSHIDA, M., et al., Nucl. Fusion **49**, (2009) 115208.
[9] HONDA, M., et al., J. Plasma Fusion Res. SERIES, **8**, (2009) 316.
[10] CALLEN, J. D., Phys. Plasmas **16**, (2009) 082504.
[11] DIAMOND, P. H., et al., Nucl. Fusion **49**, (2009) 045002.